

Leishmania donovani Requires Functional Cdc42 and Rac1 To Prevent Phagosomal Maturation

M. Lerm,^{†*} Å. Holm,[†] Å. Seiron, E. Särndahl, K.-E. Magnusson, and B. Rasmusson

Division of Medical Microbiology, Department of Molecular and Clinical Medicine, Faculty of Health Sciences, Linköping University, SE-581 85 Linköping, Sweden

Received 20 October 2005/Returned for modification 28 November 2005/Accepted 1 February 2006

***Leishmania donovani* promastigotes survive inside macrophage phagosomes by inhibiting phagosomal maturation. The main surface glycoconjugate on promastigotes, lipophosphoglycan (LPG), is crucial for survival and mediates the formation of a protective shell of F-actin around the phagosome. Previous studies have demonstrated that this effect involves inhibition of protein kinase C α . The present study shows that functional Cdc42 and Rac1 are required for the formation of F-actin around *L. donovani* phagosomes. Moreover, we present data showing that phagosomes containing LPG-defective *L. donovani*, which is unable to induce F-actin accumulation, display both elevated levels of periphagosomal F-actin and impaired phagosomal maturation in macrophages with permanently active forms of Cdc42 and Rac1. We conclude that *L. donovani* engages Cdc42 and Rac1 to build up a protective coat of F-actin around its phagosome to prevent phagosomal maturation.**

The protozoan parasite *Leishmania donovani*, the causative agent of visceral leishmaniasis, is transmitted to humans through bites by infected sand flies. Flagellated *Leishmania* promastigotes are phagocytosed by host macrophages, where they survive inside phagosomes (9, 27). Lipophosphoglycan (LPG), which is the major surface glycoconjugate of promastigotes, is essential for intracellular survival (10, 15, 23, 30). Phagosomes containing *L. donovani* mutants that lack the repeating sugars of LPG (*lpg2*^{-/-} knockout [KO]) proceed through the phagolysosomal pathway, and the parasites are killed (10). The mechanism by which LPG arrests phagosomal maturation in macrophages is partially clarified and includes accumulation of F-actin around newly formed phagosomes (17). The effects of LPG on actin are in part related to inhibition of protein kinase C α (PKC α), an enzyme implicated in F-actin depolymerization at the phagosomal membrane (2, 16, 17, 23, 25).

Results from our group indicate that LPG from *L. donovani* interacts with GM1-enriched lipid microdomains (lipid rafts, detergent-resistant membranes) in the macrophage plasma membrane and that active PKC α colocalizes to a lesser degree with GM1 in these cells (unpublished data). Moreover, it was recently shown that LPG causes a disorganization of the phagosomal membrane, preventing normal assembly of GM1-enriched microdomains (8). In line with this, we found that disrupting membrane microdomains by cholesterol depletion, thereby mimicking the effect of LPG, raised the levels of periphagosomal F-actin around LPG-deficient *lpg2*^{-/-} KO mutants. However, the levels of periphagosomal F-actin in cholesterol-depleted cells did not reach the levels observed around wild-type (WT) promastigotes (unpublished data).

The present study investigates the involvement of the Rho

family members Cdc42 and Rac1 in the generation of the F-actin shell formed around phagosomes containing *L. donovani* promastigotes. The Rho family of small GTPases, including Rho, Rac, and Cdc42, has emerged as main regulators of the cytoskeleton (11, 14). GTP-bound Rho GTPases drive cellular processes such as cytoskeletal reorganization, migration, and proliferation (7, 14, 28). Importantly, Rho GTPases play a profound role in phagocytosis of opsonized prey (6, 22, 26, 29); however, their role in nonopsonic phagocytosis is poorly understood.

Dominant negative (N17) and constitutively active (V12) forms of Cdc42 and Rac1, expressed as fusion proteins with the human immunodeficiency virus-derived cell permeable peptide TAT, were used to study the effects of these proteins on periphagosomal F-actin and phagosomal maturation in RAW264.7 macrophages. We found that simultaneous introduction of N17Cdc42 and N17Rac1 prevented the accumulation of F-actin around phagosomes with WT *L. donovani*. Conversely, introduction of V12Cdc42 and V12Rac1 restored the accumulation of periphagosomal F-actin around phagosomes with LPG-defective promastigotes, resulting in inhibition of phagosomal maturation. Interestingly, introduction of N17Cdc42 and N17Rac1 into the cells, which reduced the levels of periphagosomal F-actin around WT *L. donovani*, did not promote maturation of these phagosomes. This result points toward a direct role for Cdc42 and Rac1 in phagosomal maturation. In conclusion, our results show that *L. donovani* requires functional Cdc42 and Rac1 to build up a coat of F-actin around its phagosome to prevent phagosomal maturation.

MATERIALS AND METHODS

Cells. The murine macrophage cell line RAW264.7 was cultured at 37°C and 5% CO₂ in Dulbecco's modified Eagle medium supplemented with 10% heat-inactivated sterile-filtered fetal calf serum, 10 mM HEPES, pH 7.3, 100 U/ml penicillin, and 100 μ g/ml streptomycin (all from Gibco BRL/Life Technologies) and used for experiment between passages 3 and 10. For microscopy, 2 \times 10⁵ cells were seeded on sterile glass coverslips placed in four-well plates and grown overnight. For flow cytometry, 5 \times 10⁵ cells were seeded in 12-well plates and grown overnight.

* Corresponding author. Mailing address: Division of Medical Microbiology, Department of Molecular and Clinical Medicine, Faculty of Health Sciences, Linköping University, SE-581 85 Linköping, Sweden. Phone: 46 13 22 47 79. Fax: 46 13 22 47 89. E-mail: marle@imk.liu.se.

[†] M.L. and Å.H. contributed equally.

Parasites. WT *L. donovani* promastigotes and the isogenic LPG-defective mutant *lpg2^{-/-}* KO, both expressing green fluorescent protein (GFP), were cultured at 26°C in modified M199 medium with 500 µg/ml G418 (all from Gibco BRL/Life Technologies) as previously described (17). Expression of GFP was assessed by fluorescence microscopy. The promastigotes were used in the stationary phase of growth. Fresh medium was supplied the day before the experiment.

Transduction of RAW264.7 cells with TAT constructs. The pTAT-HA vector (where HA is hemagglutinin), TAT-N17Cdc42, and TAT-V12Cdc42 were kind gifts from Steve Dowdy. N17Rac1 and V12Rac1 were amplified from pEGFP-N17Rac1 and pEGFP-V12Rac1 using the following primers: sense, 5'-TATGCGGGTACCA TGCAGGCCATCAAGTGTGTGGTGG-3'; antisense, 5'-CTAGTCCGAATTCCT AGAGGAGGCTGCAGGCGCGC-3'. The primers were designed to carry restriction sites for KpnI and EcoRI, which were used for subcloning into the pTAT-HA vector. After the correct sequences were verified, the plasmids were transformed into *Escherichia coli* strain B121(DE3) (Novagen), and colonies expressing the plasmids were identified. Large-scale purifications were performed in Luria broth containing 50 µg/ml ampicillin and 0.1 mM IPTG (isopropyl-β-D-thiogalactopyranoside). The bacteria were collected by centrifugation (5,000 × g for 10 min at 4°C), lysed in buffer Z (8 M urea, 10 mM imidazole), sonicated, and centrifuged (18,000 × g for 10 min at 4°C). The supernatants were loaded onto Ni-nitrilotriacetic acid agarose (QIAGEN) for affinity purification of His₆-tagged TAT-Cdc42 and TAT-Rac1. The columns were washed with 25 bed volumes of buffer Z before elution of the proteins with increasing concentrations of imidazole (0.1, 0.25, 0.5, and 1.0 M) in buffer Z. The eluted fractions were checked for protein concentration using Bradford reagent (Sigma), and the protein-containing fractions were pooled and loaded on a PD-10 column (Pharmacia), which had been equilibrated with a buffer containing 50 mM Tris, pH 7.4, and 10% glycerol. The same buffer was used to elute the proteins, which were aliquoted on ice and stored at -70°C. Contaminating lipopolysaccharide was estimated to 5 to 20 ng/ml (experimental concentration) as measured by the *Limulus* assay (Coatech). To avoid unwanted effects of lipopolysaccharide, the protein preparations were preincubated with polymyxin B (Sigma) in a 10- to 100-fold molar excess (60 min on ice). To exclude possible effects of polymyxin B, equal amounts of the substance were added to the control cells. The cells were incubated with 200 nM TAT-GTPase for 30 min at 37°C. When two TAT constructs were transduced simultaneously, a 100 nM concentration of each TAT-GTPase was added to the cells. The effective transduction of the GTPases into the cells was verified by Western blotting of lysates of TAT-Cdc42- or TAT-Rac1-transduced cells using an antibody directed toward the HA epitope (Santa Cruz Biotechnology) of the fusion proteins and a horseradish peroxidase-conjugated goat anti-rabbit antibody (Dako) with an ECL Western blotting system (Amersham). To estimate the ratio of cells positive for TAT transduction, the fusion proteins (4 µM) were preincubated with a fluorescein isothiocyanate (FITC)-conjugated Fab fragment directed toward the HA epitope (20 µg/ml; Roche) for 30 min on ice before the preparations were added to the cells (final concentration of the FITC-conjugated Fab fragment, 1 µg/ml). In a control experiment, the cells were treated with the Fab fragment alone. After a 30-min incubation at 37°C, the cells were washed, fixed, and mounted for microscopy. Images were captured with the confocal microscope as described below. The ratio of cells positive for FITC staining was calculated from the evaluation of 100 to 200 cells per preparation. In the control preparations, no positive cells were found.

Infection and F-actin labeling. For infection, stationary phase *L. donovani* promastigotes were resuspended in cell culture medium and added to the cells at a parasite-to-cell ratio of 10:1, followed by a 50-min incubation at 37°C and fixation for 15 min at 4°C in 2.0% (wt/vol) paraformaldehyde (Sigma) in Krebs-Ringer glucose buffer with 1 mM Ca²⁺ and Mg²⁺. To analyze F-actin kinetics, the promastigotes were first allowed to adhere to the cells for 20 min at 37°C (pulse); this was followed by a washing step to remove unbound prey, and incubation was continued for 10, 30, or 60 min (chase) before fixation. Fixed cells were washed three times in phosphate-buffered saline (PBS; pH 7.3) with 1% bovine serum albumin (BSA; Boehringer-Mannheim) and incubated for 30 min in the same buffer at room temperature to block nonspecific binding of phalloidin. F-actin was labeled with AlexaFluor 594-phalloidin (Molecular Probes), diluted 1:40 from a stock solution (200 U/ml in methanol) in PBS, pH 7.3, with 100 µg/ml of lysophosphatidylcholine (Sigma) as a membrane-permeabilizing agent. After labeling, the cells were washed three times in PBS with 1% BSA and mounted in DAKO Antifade (Dakopatts).

LAMP1 labeling. Fixed preparations were washed in PBS, pH 7.6. The cells were permeabilized, and nonspecific binding was blocked by incubation in PBS, pH 7.6, with 2% BSA, 10% normal goat serum (Dakopatts), and 0.1% saponin (Sigma) for 30 min at room temperature, followed by washing in PBS, pH 7.6, with 2% BSA (buffer A). The preparations were incubated for 45 min at room

temperature with monoclonal rat antibodies (1DB4 diluted 1:200; Developmental Studies Hybridoma Bank, Iowa City, Iowa) against lysosome-associated membrane protein 1 (LAMP1). After being washed in buffer A, the cells were incubated for 30 min at room temperature with 200 ml/cover slip of AlexaFluor 594-conjugated goat anti-rat (Molecular Probes), diluted 1:400 in buffer A. After being washed in buffer A, the cells were mounted in DAKO Antifade (Dakopatts). Antibody 1DB4 was replaced with purified rat immunoglobulin G to control for nonspecific labeling.

Confocal microscopy. Confocal imaging was performed in a Sarastro 2000 confocal system (Molecular Dynamics) equipped with dual detectors and a Nikon microscope with a 60× oil immersion objective (numerical aperture, 1.4). The 488 and 514 lines of the argon laser were used for parallel activation of GFP/FITC and AlexaFluor 594, respectively. Dichroic mirrors with cutoff wavelengths of 535 and 595 nm were used for the excited and emitted light, respectively. A 540DF30-nm band pass filter was used for detection of GFP/FITC, and a 600-nm long pass emission filter was used for detection of AlexaFluor 594. This filter setup ensured negligible red fluorescence in the green channel and vice versa. Internalized prey was identified by careful scanning up and down, and the horizontal section was positioned in the middle of the internalized prey. This allows (i) discrimination between attached and ingested prey and (ii) assessment of the structure of both cortical and phagosome-associated F-actin. A similar approach has been employed by others to distinguish between external (attached) and internalized particles (19, 31).

Analysis of phagocytic capacity. Following TAT treatment and infection, WT and LPG-defective parasites were treated with trypsin-EDTA at 37°C for 45 min to cleave extracellular parasites. This method has previously been used by other groups as a measure for internalization of microbes (32, 33). Cells were fixed with 2% paraformaldehyde and washed several times before flow cytometry was performed on a FACSCalibur (Becton Dickinson) instrument. A preset forward scatter and side scatter was used, and GFP fluorescence was analyzed in the FL-1 channel. A total of 10,000 cells per sample were counted. The population that was positive for GFP fluorescence was clearly separated from the control population, and the gates were applied accordingly. Data analysis of the percentage of the fluorescence-positive population of the total cell population (i.e., the ratio of phagocytosing cells) and the fluorescence intensity of the positive population (corresponding to the number of internalized prey) was performed. The phagocytic capacity of the cells varied between the days of experiment (7 to 30% of the total cell population was found positive for trypsin-EDTA-resistant fluorescence); hence, the results were normalized to the phagocytic capacity of the WT in the individual experiments. Data are expressed as the means ± standard error of the means (SEM) of three independent experiments.

Measurement of periphagosomal and cortical F-actin. Periphagosomal F-actin was quantified from randomly scanned confocal images of AlexaFluor 594-phalloidin-labeled samples containing GFP-expressing promastigotes, as described by Holm et al. (17). In short, phagosomes containing promastigotes were identified in red/green images. Once phagosomes were identified, the red (F-actin) and green (GFP) channels were separated, and only the red channel was used for quantification. This procedure ensured that only structures containing internalized promastigotes, i.e., phagosomes, were studied. For quantification of periphagosomal F-actin, the F-actin rim around individual phagosomes (Periphagosomal F-actin) was manually traced in the confocal image, the fluorescence intensity profile along the trace was recorded, and the median intensity of the profile was calculated. To compensate for possible variations in instrument performance between experiment days, all results were normalized against data from phagosomes in control cells phagocytosing WT *L. donovani* promastigotes. A Student's *t* test was used for statistical analysis (18). Cortical F-actin was assessed in the same way, except that the cortical F-actin was traced.

Analysis of LAMP1 translocation to phagosomes. The translocation of LAMP1 to individual phagosomes was examined in randomly scanned confocal images. After phagosomes containing promastigotes were identified, the translocation of LAMP1 to the phagosome was classified as strong, positive, intermediate, or negative. The experiment was performed four times with similar results. A normal test and a chi-squared test for large contingency tables ($r \times c$ tables, where r is the number of rows and c is the number of columns) were used for statistical analysis (18). To facilitate analysis, the numbers of phagosomes showing intermediate, positive, and strong translocation were added together for each condition.

RESULTS AND DISCUSSION

LPG regulates the levels of periphagosomal F-actin in RAW264.7 cells. To analyze the levels of periphagosomal

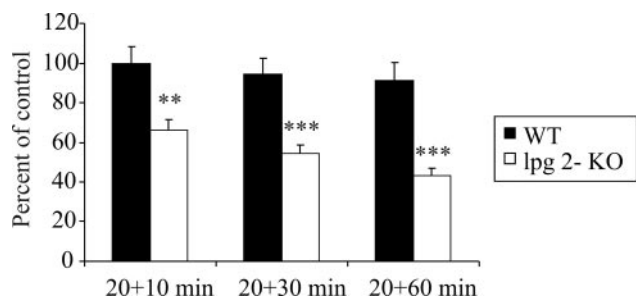


FIG. 1. Effect of LPG on the kinetics of F-actin around *L. donovani*-containing phagosomes. RAW264.7 macrophages grown on glass coverslips were allowed to interact with GFP-expressing WT *L. donovani* or LPG-defective mutants (*lpg2*^{-/-} KO) for 20 min (pulse), followed by a wash and continued incubation for 10, 30, and 60 min (chase). Following fixation, the cells were labeled with AlexaFluor 594-phalloidin and imaged in a confocal microscope. F-actin was measured by manually tracing the rim of F-actin around randomly scanned phagosomes. Shown are the mean values of the median intensity of individual traces. Each group contains data from 44 to 72 *L. donovani*-containing phagosomes from duplicate preparations made on two to three independent occasions. All results were normalized against data from cells phagocytosing WT *L. donovani* at 20+10 min. Error bars indicate SEM.

F-actin following internalization of *L. donovani* WT promastigotes or LPG-defective mutants (*lpg2*^{-/-} KO), RAW264.7 macrophages were first incubated with the promastigotes for 20 min (pulse), during which time the highly motile promastigotes attached to the macrophage surface (10, 17). Unbound prey was thereafter removed by washing (chase), and the cells were incubated for an additional 10, 30, or 60 min, followed by fixation and staining. Careful confocal scanning up and down through the cells showed that the majority of both WT and LPG-defective parasites were internalized. Thus, by positioning the horizontal confocal section in the middle of the prey, we could assess the structure of F-actin around the phagosome and distinguish it from the cortical or cell membrane-associated cortical F-actin.

Analysis of the confocal images revealed a progressive decrease of periphagosomal F-actin around phagosomes containing *lpg2*^{-/-} KO mutants (66% [$P < 0.01$] of WT [10 min] and 43% [$P < 0.001$] of WT [10 min] at 10 and 60 min, respectively), whereas the levels of F-actin around phagosomes containing WT *L. donovani* remained at a constant, high level throughout the course of incubation (Fig. 1). We did not detect any progressive increase in the amount of F-actin around the *L. donovani* phagosomes in the RAW264.7 macrophages, which is in contrast to our previous findings with J774.A1 macrophages (17). Considering that RAW264.7 and J774.A1 are two separate cell lines that differ in the level of maturity and probably also in uptake kinetics, this result is not surprising. The maintenance of cellular F-actin structures is a dynamic process involving continuous buildup and breakdown of F-actin. Therefore, small variations in actin regulatory proteins in different cell types may influence the total F-actin levels of the individual cell line. The phagocytic cups of RAW264.7 cells are generally more actin rich compared to J774.A1 cells (unpublished observation). This means that these cells have more periphagosomal F-actin from the start, which could explain why the periphagosomal F-actin does not further increase in RAW264.7.

Cdc42 and Rac1 modulate F-actin around *L. donovani*-containing phagosomes. We used the TAT-mediated protein transduction technique (1, 4, 24, 36) to deliver dominant negative and constitutively active mutants of Cdc42 and Rac1 into RAW264.7 macrophages. The cells were transduced with a 200 nM concentration of TAT-N17Cdc42 or TAT-N17Rac1 (dominant negative mutants) or both (100 nM each). The entry of the GTPases into the cells was verified by Western blotting and an immunostaining protocol using antibodies and Fab fragments, respectively, directed toward the HA-epitope of the fusion proteins as described in Materials and Methods (data not shown). Analysis of the ratio of TAT-positive cells showed that around 80% of the population was effectively transduced (data not shown), with only slight variations between the different preparations. Several studies have shown that Cdc42 and Rac1 are required for efficient phagocytosis (6, 22, 26, 29). Therefore, we determined the capacity of cells transduced with dominant negative forms of Cdc42 and Rac1 to phagocytose unopsonized WT or LPG-defective *L. donovani* by using a flow cytometry-based method, as described in Materials and Methods. In this experiment, WT or LPG-defective *L. donovani* parasites were added to untransduced cells or cells transduced with V12Cdc42, V12Rac1, N17Cdc42, N17Rac1, or with the combined treatment of N17Cdc42 and N17Rac1. The percentage of cells positive for GFP fluorescence varied between the days of the experiments (7 to 30% of the total population) (data not shown). No significant differences in phagocytic capacity between WT or LPG-defective parasites or any of the treatments could be observed (Fig. 2A), showing that internalization occurred effectively in all treatments. This result demonstrates that, in contrast to the phagocytic process described for many opsonized microorganisms, the entry of nonopsonized *L. donovani* is independent of Rac1 and Cdc42.

Next, the levels of F-actin around randomly scanned individual phagosomes in the preparations were measured. We observed significantly reduced levels of F-actin around phagosomes containing WT *L. donovani* in cells transduced with either dominant negative Cdc42 or Rac1 compared to the phagosomes in untransduced cells (54% [N17Cdc42] and 36% [N17Rac1], respectively; $P < 0.001$) (Fig. 2B and C). In cells with both N17Cdc42 and N17Rac1, the levels of F-actin around phagosomes containing WT *L. donovani* were decreased to levels comparable to the levels observed around LPG-defective mutants (23% and 25% of the phagosomes in untransduced cells, respectively) (Fig. 2B and C). This indicates that both Cdc42 and Rac1 are required for a fully developed F-actin coat around an *L. donovani*-containing phagosome. During the preparation of this report, a study was published that supports our finding that Cdc42 plays a key role in the maintenance of the F-actin coat around phagosomes containing WT *L. donovani* (20).

Since our experiments indicated that the accumulation of F-actin around *L. donovani*-containing phagosomes was dependent on functional Cdc42 and Rac1, we speculated that the coat of F-actin around phagosomes containing LPG-defective mutants would be restored in cells transduced with activated Cdc42 and Rac1. Indeed, we found that introduction of either TAT-V12Cdc42 or TAT-V12Rac1 into cells prior to the addition of *lpg2*^{-/-} KO mutants increased the levels of F-actin around phagosomes containing the parasites to levels compa-

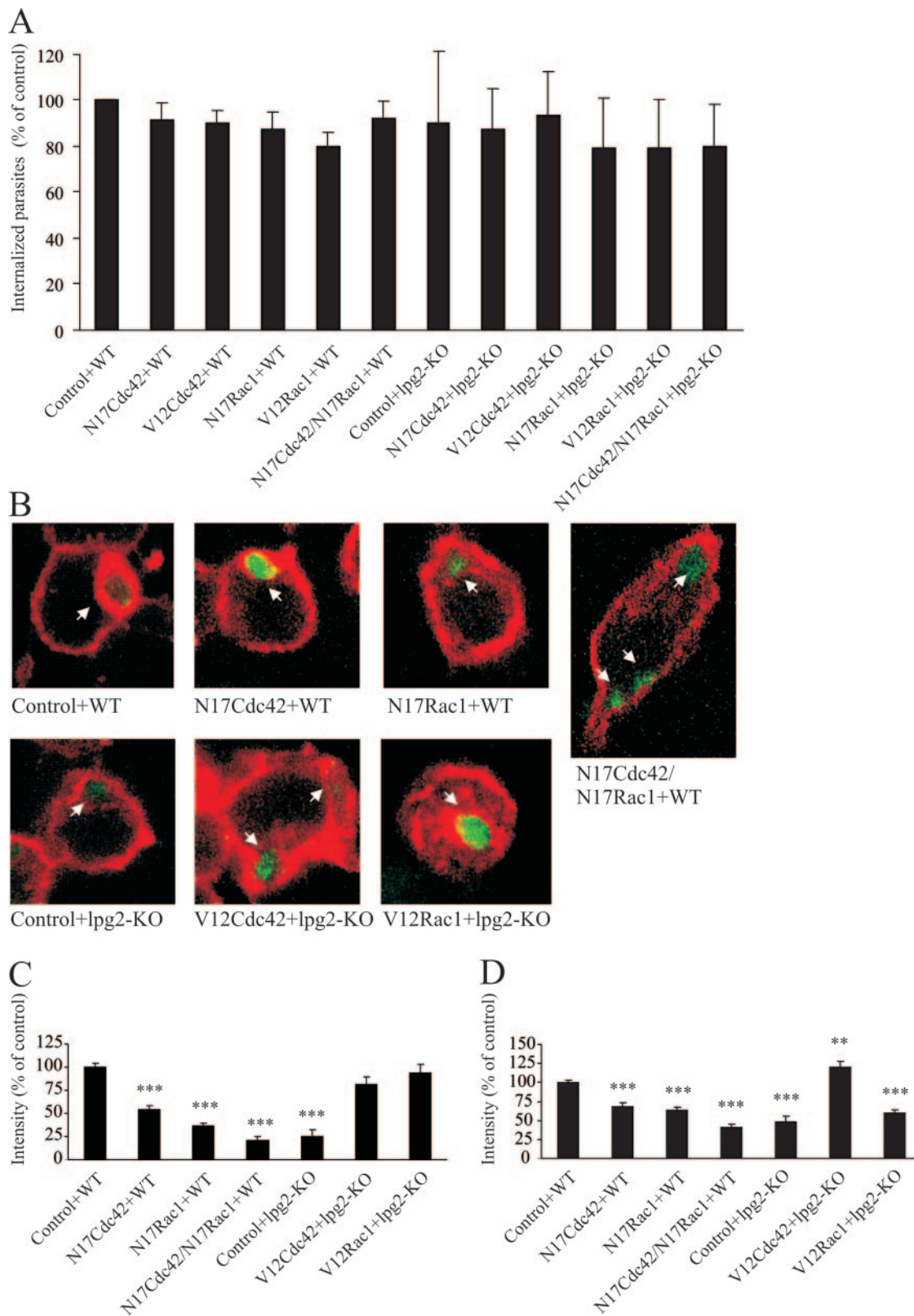


FIG. 2. F-actin around phagosomes and cortical F-actin in cells with dominant negative or constitutively active Cdc42 and Rac1. RAW264.7 macrophages were transduced with TAT-linked N17Cdc42, N17Rac1, N17Cdc42/N17Rac1 in combination, TAT-V12Cdc42, or TAT-V12Rac1. Controls were treated with buffer. Thereafter, the cells were challenged with GFP-expressing WT *L. donovani* or LPG-defective mutants (*lpq2*^{-/-} KO). (A) For flow cytometry, the cells were trypsinized and fixed after infection. The data obtained in three independent experiments represent cells positive for GFP fluorescence and are expressed as means normalized to the WT controls. (B to D) For microscopy, the cells were fixed,

rable to those measured around phagosomes with WT *L. donovani* (81% and 94% of the phagosomes in untransduced cells, respectively) (Fig. 2B and C).

To assess the effect of the transduced proteins on the overall F-actin content in cells challenged with WT or LPG-defective *L. donovani*, cortical F-actin was quantified. We observed lower levels of F-actin in cells transduced with either TAT-N17Cdc42 or TAT-N17Rac1 or with the combination of TAT-N17Cdc42/TAT-N17Rac1 and in cells challenged with *lpg2*^{-/-} KO mutants compared to untransduced cells challenged with WT *L. donovani* (69%, 64%, 41%, and 49%, respectively; $P < 0.001$) (Fig. 2D). The levels of cortical F-actin observed in cells transduced with TAT-V12Cdc42 and challenged with the LPG-defective mutant was even higher than in untransduced cells challenged with WT *L. donovani* (21%; $P < 0.005$), but this effect was not found in cells transduced with TAT-V12Rac1 (Fig. 2D). We have previously shown that the amount of cortical F-actin in cells challenged with *lpg2*^{-/-} KO mutants does not differ from noninfected cells, whereas WT *L. donovani* increases the amount of cortical F-actin (17). The observation that permanently activated Cdc42, but not permanently activated Rac1, increases cortical F-actin is supported by an experiment performed on human neutrophils, which shows a strong ring of cortical F-actin only in the presence of active Cdc42 (5). This suggests that cells with manipulated Cdc42 and Rac1 functions display specific traits, and thus the modulation of periphagosomal F-actin with the activated forms of these GTPases is not simply a result of increased total F-actin in the cell.

Activation of Cdc42 and Rac1 inhibits translocation of LAMP1 to phagosomes. Previous studies have shown that a coat of F-actin around *L. donovani* phagosomes prevents phagosomal maturation. Therefore, we investigated whether activation of Cdc42 and Rac1 would rescue the LPG-defective *lpg2*^{-/-} KO mutant from being destroyed in a phagolysosomal compartment. We quantified the number of phagosomes positive for the late endosomal marker LAMP1 as a measure for phagosomal maturation (16). In short, the cells were transduced with TAT-V12Cdc42 or TAT-V12Rac1 and infected with the *lpg2*^{-/-} KO mutant. The cells were thereafter fixed and stained with antibodies directed toward LAMP1 and examined in the confocal microscope. Translocation of LAMP1 to the phagosomes was classified as strong, positive, intermediate, or negative. As previously described (17), we found that translocation of LAMP1 to phagosomes containing WT *L. donovani* was significantly reduced compared to phagosomes with *lpg2*^{-/-} KO mutants, indicating defective phagosomal maturation ($P < 0.001$). In cells transduced with TAT-V12Cdc42 or TAT-V12Rac1, translocation of LAMP1 to phagosomes with *lpg2*^{-/-} KO mutants was reduced to the same level as with WT *L. donovani*, showing that activation of Cdc42 or Rac1 is sufficient to prevent the LPG-defective mutants from entering the phagolysosomal

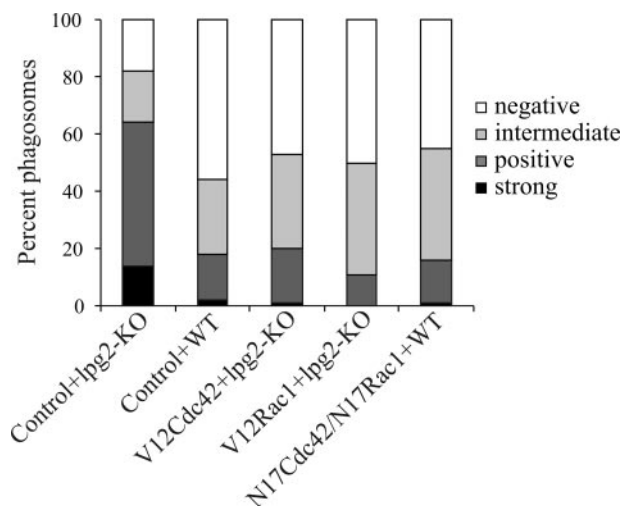


FIG. 3. Translocation of LAMP1 to phagosomes in cells with dominant negative or constitutively active Cdc42 and Rac1. RAW264.7 macrophages grown on glass coverslips were transduced with TAT-linked N17Cdc42, N17Rac1, N17Cdc42/N17Rac1 complex, TAT-V12Cdc42, or TAT-V12Rac1. Controls were incubated with buffer. The cells were then allowed to interact with GFP-expressing WT *L. donovani* or LPG-defective mutants (*lpg2*^{-/-} KO). Following fixation, the cells were fluorescently labeled using the antibody IDB4 directed to LAMP1, and random areas were imaged by confocal microscopy. The images were evaluated with respect to the translocation of LAMP1 to individual phagosomes, which was classified as strong, positive, intermediate, or negative. The graph shows data from one representative experiment of four, where 109 to 154 phagosomes were examined.

pathway. Interestingly, the reverse experiment using TAT-N17Cdc42 or TAT-N17Rac1 with WT *L. donovani* did not enhance the translocation of LAMP1 to WT-containing phagosomes compared to untransduced cells (Fig. 3).

The prevention of LAMP1 translocation in cells transduced with constitutively active Cdc42 or Rac1 correlates well with the accumulation of F-actin seen around the phagosomes in these cells (Fig. 2A and B). Several studies in similar and other systems have linked disassembly of periphagosomal F-actin to phagosomal maturation (2, 13, 16, 17). The exact mechanism by which the buildup of an F-actin coat around a phagosome inhibits phagosomal maturation is still not fully resolved, but it is possible that the fusion of the endosomes with the phagosome is physically prevented due to the abundant, interwoven actin filaments surrounding the phagosome (16, 17, 21, 27).

Although simultaneous inhibition of Cdc42 and Rac1 reduced the amount of periphagosomal F-actin around phagosomes containing WT *L. donovani* to levels comparable to phagosomes with LPG-defective mutants, the translocation of LAMP1 to these phagosomes was still prevented (Fig. 3). Although surprising at first glance, this result may reflect a recently identified mechanism for lysosome movement. There

labeled with AlexaFluor 594-phalloidin, and imaged in a confocal microscope. Representative images of phalloidin-stained RAW264.7 macrophages infected with *L. donovani* are shown in panel B. F-actin was measured by manually tracing the rim of F-actin around randomly scanned phagosomes (101 to 338 measured phagosomes from duplicate preparations and at least three independent occasions) (C) or the F-actin at the cell periphery (50 to 75 measurements from duplicate preparations and three independent occasions) (D). Shown are the mean values of the median intensity of individual traces. The results in panels C and D were normalized against data from control cells with WT *L. donovani*. Error bars are SEM.

are several lines of evidence suggesting that endosomes and lysosomes move through the cytoplasm in a *Listeria*-like manner by the formation of actin-based comet tails (3, 12, 34, 35). In fact, a recent report showed that the formation of comet tails on endosomes is dependent on Cdc42 and the Cdc42 effector protein, Wiskott-Aldrich syndrome protein (35). In addition, the movement of lysosomal compartments in HL60 cells is blocked by dominant negative Cdc42 but functions normally in cells with constitutively active Cdc42 (unpublished data). The mechanisms by which dominant negative forms of Cdc42 and Rac1 prevent phagosomal maturation will be the subject of future studies.

As mentioned in the introduction to this report, we had preliminary indications that additional mechanisms besides the inhibition of PKC α are involved in the LPG-induced buildup of periphagosomal F-actin. Here we identified activation of Cdc42 and Rac1 as important coplayers in *L. donovani* pathogenesis. Our results show that LPG signals through Rac1 and Cdc42 to form a shell of F-actin around phagosomes required for intracellular survival of *L. donovani*. The relative importance of PKC α versus Cdc42 and Rac1 during *L. donovani* infection needs further analysis.

ACKNOWLEDGMENTS

We are grateful to Albert Descoteaux for the *Leishmania* parasites and to Steve Dowdy for the pTAT-HA plasmids. The monoclonal LAMP1 antibody developed by J. T. August was obtained from the Developmental Studies Hybridoma Bank, developed under the auspices of the National Institute of Child Health and Human Development and maintained by the University of Iowa, Department of Biological Sciences, Iowa City, Iowa.

The project was financially supported by Swedish Medical Research Council grants 6251 (K.E.M.) and 12725 (E.S.); Swedish Research Council grants 621-2001-3570 (K.E.M.), 521-2002-6393 (B.R.), and 529-2003-5994 (M.L.); the Swedish Society for Medical Research (B.R. and M.L.); the Swedish Medical Association (B.R. and M.L.); Magn. Bergvalls Stiftelse (B.R.); and Stiftelsen Lars Hiertas Minne (B.R.).

REFERENCES

- Alblas, J., L. Ulfman, P. Hordijk, and L. Koenderman. 2001. Activation of Rho and ROCK are essential for detachment of migrating leukocytes. *Mol. Biol. Cell* **12**:2137–2145.
- Allen, L. H., and A. Aderem. 1995. A role for MARCKS, the alpha isozyme of protein kinase C and myosin I in zymosan phagocytosis by macrophages. *J. Exp. Med.* **182**:829–840.
- Apodaca, G. 2001. Endocytic traffic in polarized epithelial cells: role of the actin and microtubule cytoskeleton. *Traffic* **2**:149–159.
- Becker-Hapak, M., S. S. McAllister, and S. F. Dowdy. 2001. TAT-mediated protein transduction into mammalian cells. *Methods* **24**:247–256.
- Bird, M. M., G. Lopez-Lluch, A. J. Ridley, and A. W. Segal. 2003. Effects of microinjected small GTPases on the actin cytoskeleton of human neutrophils. *J. Anat.* **203**:379–389.
- Caron, E., and A. Hall. 1998. Identification of two distinct mechanisms of phagocytosis controlled by different Rho GTPases. *Science* **282**:1717–1721.
- Chimini, G., and P. Chavrier. 2000. Function of Rho family proteins in actin dynamics during phagocytosis and engulfment. *Nat. Cell Biol.* **2**:E191–E196.
- Dermine, J. F., G. Goyette, M. Houde, S. J. Turco, and M. Desjardins. 2005. *Leishmania donovani* lipophosphoglycan disrupts phagosome microdomains in J774 macrophages. *Cell Microbiol.* **7**:1263–1270.
- Descoteaux, A., and S. J. Turco. 2002. Functional aspects of the *Leishmania donovani* lipophosphoglycan during macrophage infection. *Microbes Infect.* **4**:975–981.
- Desjardins, M., and A. Descoteaux. 1997. Inhibition of phagolysosomal biogenesis by the *Leishmania* lipophosphoglycan. *J. Exp. Med.* **185**:2061–2068.
- Etienne-Manneville, S., and A. Hall. 2002. Rho GTPases in cell biology. *Nature* **420**:629–635.
- Fehrenbacher, K., T. Huckaba, H. C. Yang, I. Boldogh, and L. Pon. 2003. Actin comet tails, endosomes and endosymbionts. *J. Exp. Biol.* **206**:1977–1984.
- Greenberg, S., J. el Khoury, F. di Virgilio, E. M. Kaplan, and S. C. Silverstein. 1991. Ca²⁺-independent F-actin assembly and disassembly during Fc receptor-mediated phagocytosis in mouse macrophages. *J. Cell Biol.* **113**:757–767.
- Hall, A. 1998. Rho GTPases and the actin cytoskeleton. *Science* **279**:509–514.
- Handman, E., L. F. Schnur, T. W. Spithill, and G. F. Mitchell. 1986. Passive transfer of *Leishmania* lipopolysaccharide confers parasite survival in macrophages. *J. Immunol.* **137**:3608–3613.
- Holm, A., K. Tejle, T. Gunnarsson, K. E. Magnusson, A. Descoteaux, and B. Rasmusson. 2003. Role of protein kinase C alpha for uptake of unopsonized prey and phagosomal maturation in macrophages. *Biochem. Biophys. Res. Commun.* **302**:653–658.
- Holm, A., K. Tejle, K. E. Magnusson, A. Descoteaux, and B. Rasmusson. 2001. *Leishmania donovani* lipophosphoglycan causes periphagosomal actin accumulation: correlation with impaired translocation of PKC α and defective phagosome maturation. *Cell Microbiol.* **3**:439–447.
- Kirkwood, B. 1992. *Essentials of medical statistics*. Blackwell Scientific Publications, Oxford, United Kingdom.
- Le Poole, I. C., R. M. van den Wijngaard, W. Westerhof, R. P. Verkruijsen, R. P. Dutrieux, K. P. Dingemans, and P. K. Das. 1993. Phagocytosis by normal human melanocytes in vitro. *Exp. Cell Res.* **205**:388–395.
- Lodge, R., and A. Descoteaux. 2005. *Leishmania donovani* promastigotes induce periphagosomal F-actin accumulation through retention of the GTPase Cdc42. *Cell Microbiol.* **11**:1647–1658.
- Lodge, R., and A. Descoteaux. 2005. Modulation of phagolysosome biogenesis by the lipophosphoglycan of *Leishmania*. *Clin. Immunol.* **114**:256–265.
- Massol, P., P. Montcourrier, J. C. Guillemot, and P. Chavrier. 1998. Fc receptor-mediated phagocytosis requires CDC42 and Rac1. *EMBO J.* **17**:6219–6229.
- McNeely, T. B., and S. J. Turco. 1990. Requirement of lipophosphoglycan for intracellular survival of *Leishmania donovani* within human monocytes. *J. Immunol.* **144**:2745–2750.
- Myou, S., X. Zhu, E. Boetticher, S. Myo, A. Meliton, A. Lambertino, N. M. Munoz, and A. R. Leff. 2002. Blockade of focal clustering and active conformation in beta 2-integrin-mediated adhesion of eosinophils to intercellular adhesion molecule-1 caused by transduction of HIV TAT-dominant negative Ras. *J. Immunol.* **169**:2670–2676.
- Ng Yan Hing, J. D., M. Desjardins, and A. Descoteaux. 2004. Proteomic analysis reveals a role for protein kinase C-alpha in phagosome maturation. *Biochem. Biophys. Res. Commun.* **319**:810–816.
- Olazabal, I. M., E. Caron, R. C. May, K. Schilling, D. A. Knecht, and L. M. Machesky. 2002. Rho-kinase and myosin-II control phagocytic cup formation during CR, but not Fc γ R, phagocytosis. *Curr. Biol.* **12**:1413–1418.
- Rasmusson, B., and A. Descoteaux. 2004. Contribution of electron and confocal microscopy in the study of *Leishmania*-macrophage interactions. *Microsc. Microanal.* **10**:656–661.
- Ridley, A. J., and A. Hall. 1992. The small GTP-binding protein Rho regulates the assembly of focal adhesions and actin stress fibers in response to growth factors. *Cell* **70**:389–399.
- Robinson, J. M., and J. A. Badwey. 2002. Rapid association of cytoskeletal remodeling proteins with the developing phagosomes of human neutrophils. *Histochem. Cell Biol.* **118**:117–125.
- Scianimanico, S., M. Desrosiers, J. F. Dermine, S. Meresse, A. Descoteaux, and M. Desjardins. 1999. Impaired recruitment of the small GTPase rab7 correlates with the inhibition of phagosome maturation by *Leishmania donovani* promastigotes. *Cell Microbiol.* **1**:19–32.
- Simons, M. P., W. M. Nauseef, and M. A. Apicella. 2005. Interactions of *Neisseria gonorrhoeae* with adherent polymorphonuclear leukocytes. *Infect. Immun.* **73**:1971–1977.
- Sinha, B., P. Francois, Y. A. Que, M. Hussain, C. Heilmann, P. Moreillon, D. Lew, K. H. Krause, G. Peters, and M. Herrmann. 2000. Heterologously expressed *Staphylococcus aureus* fibronectin-binding proteins are sufficient for invasion of host cells. *Infect. Immun.* **68**:6871–6878.
- Sinha, B., P. P. Francois, O. Nusse, M. Foti, O. M. Hartford, P. Vaudaux, T. J. Foster, D. P. Lew, M. Herrmann, and K. H. Krause. 1999. Fibronectin-binding protein acts as *Staphylococcus aureus* invasin via fibronectin bridging to integrin $\alpha_5\beta_1$. *Cell Microbiol.* **1**:101–117.
- Southwick, F. S., W. Li, F. Zhang, W. L. Zeile, and D. L. Purich. 2003. Actin-based endosome and phagosome rocketing in macrophages: activation by the secretagogue antagonists lanthanum and zinc. *Cell Motil. Cytoskeleton* **54**:41–55.
- Taunton, J., B. A. Rowning, M. L. Coughlin, M. Wu, R. T. Moon, T. J. Mitchison, and C. A. Larabell. 2000. Actin-dependent propulsion of endosomes and lysosomes by recruitment of N-WASP. *J. Cell Biol.* **148**:519–530.
- Wadia, J. S., R. V. Stan, and S. F. Dowdy. 2004. Transducible TAT-HA fusogenic peptide enhances escape of TAT-fusion proteins after lipid raft macropinocytosis. *Nat. Med.* **10**:310–315.